

THE SEARCH FOR TOP SQUARKS AT THE FERMILAB TEVATRON COLLIDER

Howard Baer¹, John Sender² and Xerxes Tata²

¹*Department of Physics, Florida State University, Tallahassee, FL 32306 USA*

²*Department of Physics and Astronomy, University of Hawaii, Honolulu, HI 96822 USA*

(September 5, 2018)

Abstract

The lighter superpartner of the top quark (\tilde{t}_1) may be considerably lighter than squarks of the first two generations, and hence may be accessible to Tevatron collider searches, even if the other squarks and the gluino are too heavy. For the range of $m_{\tilde{t}_1}$ of interest at the Tevatron, the \tilde{t}_1 decays to a chargino via $\tilde{t}_1 \rightarrow b\tilde{W}_1$ if this is kinematically allowed; otherwise, the flavor-changing loop decay $\tilde{t}_1 \rightarrow c\tilde{Z}_1$ dominates. In the latter case, \tilde{t}_1 production is signalled by jet(s) plus \cancel{E}_T events. If, instead, the chargino decay is allowed, $1\ell + b\text{-jets} + \cancel{E}_T$ and $\ell^+\ell'^- + jet(s) + \cancel{E}_T$ events from leptonic decays of \tilde{W}_1 provide the most promising signals. We perform detailed simulations for each of these signals using ISAJET 7.07 and devise cuts to enable the extraction of each of these signals above standard model backgrounds from vector boson or top quark production. With an integrated luminosity of 100 pb^{-1} , experiments should be able to probe top squark masses up to $\sim 100\text{ GeV}$ in each of these channels; the detection of the signal in the single lepton channel, however, requires reasonable capability to tag displaced b decay vertices in the central region.

I. INTRODUCTION

The observation that precision measurements of gauge couplings at scale M_Z by the LEP experiments are consistent with the simplest supersymmetric [1] SU(5) grand unification [2] (but not with minimal *non*-supersymmetric SU(5)) has led many authors to seriously re-examine the expectations for sparticle masses [3] within this framework. More recently, several studies of the collider phenomenology of supergravity models have also appeared [4]. On the experimental side, direct constraints on such models come from non-observation of super-partners at colliding beam experiments. For instance, the non-observation of multi-jet plus missing transverse momentum (\cancel{E}_T) events above expected standard model (SM) background levels has led the CDF and D0 collaborations to conclude [5,6],

$$m_{\tilde{g}}, m_{\tilde{q}} > 100 - 150 \text{ GeV}, \quad (1)$$

where the considerable range in the bound is due to the dependence of the missing \cancel{E}_T cross section on the parameters [7] of the Minimal Supersymmetric Model (MSSM). In obtaining these mass limits, it is usually assumed that there exist ten or twelve types of mass degenerate squarks. This is usually justified by appealing to the framework of minimal supergravity models, where the sfermions are all expected to be degenerate at an ultra-high unification scale; this degeneracy is broken when these \overline{MS} mass parameters are evolved down to the electroweak scale relevant for phenomenological analyses. For the squarks of the first two generations, this evolution is dominantly governed by their (common) QCD interactions so that their masses are split only by the relatively small electroweak interactions. As a result, these remain essentially degenerate with a mass $m_{\tilde{q}}$.

In contrast, the masses of third generation squarks obtain substantial contributions [8] also from the large top family Yukawa interactions, which also induce a substantial mixing [9] between the \tilde{t}_L and \tilde{t}_R squarks. These interactions reduce the diagonal masses relative to $m_{\tilde{q}}$ in much the same way that they drive the Higgs mass squared to negative values, resulting in the breaking of electroweak symmetry. At the weak scale, the soft-breaking masses for \tilde{t} -squarks can be written in the form [10],

$$\begin{aligned} m_{\tilde{t}_L}^2 &= m_{\tilde{q}}^2 - 2f_t^2 m_0^2 \Delta_t - 2f_b^2 m_0^2 \Delta_b + m_t^2, \\ m_{\tilde{t}_R}^2 &= m_{\tilde{q}}^2 - 4f_t^2 m_0^2 \Delta_t + m_t^2. \end{aligned} \quad (2)$$

Here, $f_t = \frac{gm_t}{\sqrt{2}M_W v} \sqrt{v^2 + v'^2}$ ($f_b = \frac{gm_b}{\sqrt{2}M_W v'} \sqrt{v^2 + v'^2}$) are top (bottom) family Yukawa couplings, m_0 is the universal sfermion mass at the unification scale and $\Delta_{t,b}$ are dimensionless parameters ~ 0.1 that can be numerically computed within a model. The term involving the bottom Yukawa coupling is negligible unless $\tan\beta (= \frac{v}{v'})$ is close to m_t/m_b [11]. Assuming squarks are heavier than top quarks, we expect the mass ordering $m_{\tilde{t}_R} < m_{\tilde{t}_L} < m_{\tilde{q}}$. As already noted, \tilde{t}_L and \tilde{t}_R are mixed by their Yukawa interactions. The \tilde{t} -squark mass squared matrix takes the form,

$$\mathcal{M}_{\tilde{t}}^2 = \begin{bmatrix} m_{\tilde{t}_L}^2 + m_t^2 - M_Z^2 \cos 2\beta (-\frac{1}{2} + \frac{2}{3} \sin^2 \theta_W) & -m_t(A_t - \mu \cot \beta) \\ -m_t(A_t - \mu \cot \beta) & m_{\tilde{t}_R}^2 + m_t^2 + M_Z^2 \cos 2\beta (\frac{2}{3} \sin^2 \theta_W) \end{bmatrix}, \quad (3)$$

where A_t is the trilinear soft SUSY breaking scalar coupling evaluated at the electroweak scale and μ is the superpotential Higgs mixing term. The mass eigenstates (\tilde{t}_1 and \tilde{t}_2) can be readily obtained by diagonalizing this matrix. For the eigenvalues, we have

$$\begin{aligned}
m_{\tilde{t}_{1,2}}^2 &= \frac{1}{2}(m_{\tilde{t}_L}^2 + m_{\tilde{t}_R}^2) + \frac{1}{4}M_Z^2 \cos 2\beta + m_t^2 \\
&\mp \left\{ \left[\frac{1}{2}(m_{\tilde{t}_L}^2 - m_{\tilde{t}_R}^2) + \frac{\cos 2\beta}{12}(8M_W^2 - 5M_Z^2) \right]^2 + m_t^2(A_t - \mu \cot \beta)^2 \right\}^{\frac{1}{2}}. \quad (4)
\end{aligned}$$

The corresponding mass eigenstates are

$$\begin{aligned}
\tilde{t}_1 &= \cos \theta_t \tilde{t}_L - \sin \theta_t \tilde{t}_R, \\
\tilde{t}_2 &= \sin \theta_t \tilde{t}_L + \cos \theta_t \tilde{t}_R, \quad (5)
\end{aligned}$$

where the mixing angle θ_t is given by

$$\tan \theta_t = \frac{m_{\tilde{t}_L}^2 + m_t^2 - M_Z^2 \cos 2\beta (-\frac{1}{2} + \frac{2}{3} \sin^2 \theta_W) - m_{\tilde{t}_1}^2}{-m_t(A_t - \mu \cot \beta)}. \quad (6)$$

The freedom to adjust the soft-SUSY breaking parameter A_t enables us to fix the lighter top squark (the stop, or \tilde{t}_1) mass essentially independently of the masses of other squarks. We see that \tilde{t}_1 , which has a mass smaller than even $m_{\tilde{t}_R}$, can indeed be much lighter than the first two generations of squarks. In fact, \tilde{t}_1 can easily be as light as ~ 50 GeV even if other squarks and gluinos have masses of several hundred GeV. Although this is not directly relevant to our discussion, we also mention that SU(2) gauge invariance requires that $m_{\tilde{b}_L} = m_{\tilde{t}_L}$ (aside from D -terms) whereas $m_{\tilde{b}_R} \simeq m_{\tilde{q}}$ unless $\tan \beta$ is very large. For moderate values of $\tan \beta$, μ and A_b , \tilde{b}_L - \tilde{b}_R mixing is expected to be small so that \tilde{b}_L and \tilde{b}_R closely approximate the mass eigenstates.

Having convinced ourselves that \tilde{t}_1 can indeed be much lighter than other squarks, it is reasonable to ask what current experiments tell us about its mass. The measurement of the total width of the Z boson as well as direct searches for squarks at LEP [12] imply [13] that

$$m_{\tilde{t}_1} \gtrsim 45 \text{ GeV}. \quad (7)$$

Top squarks can also be pair produced at $p\bar{p}$ colliders, via $q\bar{q}$ and gg fusion diagrams. Unlike squarks of the first two generations, there exists no significant cross section contribution from gluino exchange diagrams, so that $\sigma(\tilde{t}_1\tilde{t}_1)$ is determined completely in terms of $m_{\tilde{t}_1}$. For stops with a mass in the 50-125 GeV range— accessible to Tevatron experiments— the dominant decay mode is expected to be the two body $\tilde{t}_1 \rightarrow b\tilde{W}_1$, if it is kinematically allowed. If instead $m_{\tilde{t}_1} < m_b + m_{\tilde{W}_1}$, then decay via flavor changing loop diagrams is expected to dominate [14], in which case $\tilde{t}_1 \rightarrow c\tilde{Z}_1$. In the latter case stop production, like squark production (but without cascade decays), would be signalled only by events with jets plus \cancel{E}_T . When the chargino decay mode is accessible, stop signatures are topologically the same as those of t -quarks. We have checked at least within the MSSM framework that if $m_{\tilde{t}_1} \lesssim 150$ GeV, the decay $\tilde{t}_1 \rightarrow bW\tilde{Z}_1$ is kinematically allowed only when the two-body decay $\tilde{t}_1 \rightarrow b\tilde{W}_1$ is also allowed. Thus the three body decay to real W bosons is never phenomenologically relevant for the discussion of \tilde{t} -squark signals at the Tevatron.

The production of \tilde{t}_1 -squark pairs at the Tevatron was studied in Ref. [15], where it was shown that $\sigma(\tilde{t}_1\tilde{t}_1) \sim (\frac{1}{5} - \frac{1}{10})\sigma(t\bar{t})$, for equal top and stop masses. These authors,

using parton level Monte Carlo programs, attempted to translate the CDF [5] squark bound Eq.(1) to a limit on the mass of \tilde{t}_1 , under the assumption that $\tilde{t}_1 \rightarrow c\tilde{Z}_1$. They concluded that the CDF data imply a stronger bound than the LEP limit in Eq. (4), but only if the lightest neutralino, also assumed to be the lightest SUSY particle (LSP), has a mass of just a few GeV. For $m_{\tilde{Z}_1} > 10$ GeV, their analysis showed that it is entirely possible that \tilde{t}_1 could have escaped detection if its mass was just above the LEP bound. These authors also studied the dilepton signal from the decay $\tilde{t}_1 \rightarrow b\tilde{W}_1, \tilde{W}_1 \rightarrow \ell\nu\tilde{Z}_1$. Since their purpose was to study whether it would be identifiable in the CDF search for top quarks, they used the corresponding CDF cuts. They found that the stop signal would be dwarfed by the corresponding signal from t -quark production.

Since that time, the CDF experiment has more than quadrupled its data sample. Furthermore, the D0 experiment has started operation and accumulated a data sample of comparable magnitude. By the end of the current run (Run I B), the combined integrated luminosity is expected to be $\gtrsim 100 pb^{-1}$; *i.e.*, $\gtrsim 25$ times larger than that used in the earlier analysis [15]. On the theoretical front, the production and decay patterns of all sparticles as given by the MSSM have been incorporated into the event simulation program ISAJET [16]. This should allow for considerably better simulation of the signals than in Ref. [15].

The purpose of this paper is to re-examine the prospects for discovering the lighter top squark at the Tevatron in the case where other squarks and gluinos are too heavy to be kinematically accessible, regardless of whether the decay $\tilde{t}_1 \rightarrow b\tilde{W}_1$ is allowed. In light of the fact that the Tevatron experiments will soon have a very large event sample, and considering the improvements in theoretical technology since the last study, we felt that a reassessment was warranted. For the \cancel{E}_T signal we improve on our earlier study in that we use a more sophisticated simulation. We will see later that the inclusion of QCD radiation in ISAJET significantly affects our conclusion about the mass reach of the Tevatron, particularly when \tilde{Z}_1 is relatively heavy. In the case when the chargino decay of the stop is kinematically allowed, we adopt a different philosophy from our earlier study. Instead of focussing on what the Tevatron top *quark* analysis can tell us about top *squarks*, we devise cuts to separate the SUSY signal from the top signal as well as from other SM backgrounds. We then find that, with an integrated luminosity of $\sim 100 pb^{-1}$, experiments at the Tevatron should be able to search for \tilde{t}_1 as heavy as about 100 GeV, even in this case.

The rest of this paper is organized as follows. We briefly describe our simulation of stop events at the Tevatron in Sec. II. In Sec. III, we investigate Tevatron signatures from $\tilde{t}_1 \rightarrow c\tilde{Z}_1$ decay, and show regions of the $m_{\tilde{t}_1}$ *vs.* $m_{\tilde{Z}_1}$ parameter space that ought to be accessible to Tevatron collider experiments. In Sec. IV, we examine both the single lepton plus jets signature as well as the dilepton plus jets signature, when $\tilde{t}_1 \rightarrow b\tilde{W}_1$ is the dominant stop decay. Again, we show regions of parameter space explorable via these modes. We conclude in Sec. V with a summary of our results along with some general remarks.

II. TOP SQUARK SIMULATION AT THE TEVATRON

We use the program ISAJET version 7.07 [16] to simulate events from the production of \tilde{t}_1 pairs at the Tevatron. Once produced, the stop rapidly decays via $\tilde{t}_1 \rightarrow b\tilde{W}_1$ if this decay is kinematically allowed; if not, we assume that it decays via $c\tilde{Z}_1$ with a branching fraction of 100%. In other words, the decay patterns of the stop are determined by sparticle

masses and do not depend on the stop or gaugino mixing angles. Furthermore, in this latter case, the \cancel{E}_T signal from stop production is completely determined in terms of $m_{\tilde{t}_1}$ and $m_{\tilde{Z}_1}$ and is independent of any other parameters. If, on the other hand, the stop is heavy enough to decay via the chargino mode, its signals obviously depend on the decay patterns of the chargino. For any set of input parameters, ISAJET then decays the daughter chargino with branching fractions as given by the MSSM. Over a large range of model parameters, the W^* -mediated amplitude dominates the decays of the chargino, so that the branching fraction for the decay $\tilde{W}_1 \rightarrow \mu\nu\tilde{Z}_1$ is about 11%. In our computations, we will use the supergravity motivated choice $\mu = -m_{\tilde{g}}$ as our default value and fix $\tan\beta = 2$. This then implies $m_{\tilde{W}_1} \simeq 2m_{\tilde{Z}_1} \simeq \frac{1}{3}m_{\tilde{g}}$, which together with the stop mass fixes the kinematics of the events. Effects from radiation off initial and final state partons, fragmentation of the c or b daughters of the stop, final state hadronization and underlying event activity are incorporated in ISAJET.

We have modelled the experimental conditions at the Tevatron by incorporating a toy calorimeter with segmentation $\Delta\eta \times \Delta\phi = 0.1 \times 0.087$ and extending to $|\eta| = 4$ in our simulation. We have assumed an energy resolution of $50\%/\sqrt{E_T}$ ($15\%/\sqrt{E_T}$) for the hadronic (electromagnetic) calorimeter. Jets are defined to be hadron clusters with $E_T > 15$ GeV within a cone of $\Delta R = \sqrt{\Delta\eta^2 + \Delta\phi^2} = 0.7$ and $|\eta_j| < 3.5$. We consider an electron (muon) to be isolated if $p_T(e) > 8$ GeV ($p_T(\mu) > 5$ GeV) and the hadronic energy in a cone with $\Delta R = 0.4$ about the lepton does not exceed $\min(\frac{1}{4}E_T(\ell), 4$ GeV). Non-isolated electrons are included as part of the accompanying hadron cluster.

III. SEARCH FOR STOP DECAY TO CHARM PLUS NEUTRALINO

When the chargino is heavier than $(m_{\tilde{t}_1} - m_b)$, the \tilde{t}_1 in the mass range of interest essentially decays [14] via $\tilde{t}_1 \rightarrow c\tilde{Z}_1$ so that stop pair production would be signalled by events with charm jet(s) together with \cancel{E}_T . In our analysis [17] of this signature, we have imposed the following CDF-inspired [5] cuts on the signal:

- (i) We require at least two jets in each event with at least one jet in the central region, $|\eta_j| \leq 1$. All jets are required to be separated by at least 30° in azimuth from $\vec{\cancel{E}}_T$.
- (ii) If $n_j = 2$, we further require $\Delta\phi(j_1, j_2) \leq 150^\circ$.
- (iii) We veto events containing leptons (from the c -jet) with $p_T(\ell) \geq 10$ GeV to reduce the background from $W \rightarrow \ell\nu$ ($\ell = e$ or μ). We have checked that this leads to very little loss of signal.
- (iv) We require $\cancel{E}_T \geq 50$ GeV [5] to reduce backgrounds from QCD heavy flavours and mismeasured jets.

SM backgrounds from heavy flavor production ($c\bar{c}$ and $b\bar{b}$) and multi-jet production (with substantial jet energy mismeasurement) are very dependent on a detailed detector simulation, but are expected [5,6] to be small, given a large enough \cancel{E}_T cut and lepton veto. The major backgrounds we consider here are from vector boson production, and include (a)

$Z \rightarrow \nu\bar{\nu}$ production, (b) $W \rightarrow \tau\nu$ production (where the hadronically decaying τ can be one of the jets), and (c) $W \rightarrow \ell\nu$, where extra jets come from initial state QCD radiation.

The \cancel{E}_T distribution, before any cuts, from stop events at a $p\bar{p}$ collider with $\sqrt{s} = 1.8$ TeV is illustrated in Fig. 1 for two representative choices of \tilde{t}_1 and \tilde{Z}_1 masses: (a) $m_{\tilde{t}_1} = 85$ GeV, $m_{\tilde{Z}_1} = 20$ GeV, and (b) $m_{\tilde{t}_1} = 125$ GeV, $m_{\tilde{Z}_1} = 40$ GeV. Also shown are the corresponding distribution from the W and Z backgrounds listed above which have been computed using ISAJET. We have used the Set I structure function of Eichten *et. al.* [18] in our computation. As expected, the $W \rightarrow \ell\nu$ background peaks at $\simeq M_W/2$, while the \cancel{E}_T spectra from the other backgrounds are softer. We see that the $\cancel{E}_T > 50$ GeV cut (*iv*) is very effective in cutting these backgrounds with a factor of ~ 2 loss of signal. Nevertheless, even after cuts (*i-iv*), the $W \rightarrow \tau$ ($Z \rightarrow \nu\nu$) background is 23 pb (12 pb) in contrast to the signal cross section of 9.2 pb and 1.9 pb for our representative cases introduced above. The lepton veto reduces the $W \rightarrow \ell\nu$ background to negligible levels. We have also checked that $Z \rightarrow \tau\bar{\tau}$ is small compared to the other backgrounds.

To facilitate further separation of the stop signal from SM background, we have studied the correlation between $\Delta\phi$, the transverse plane opening angle between $\vec{\cancel{E}}_T$ and the nearest jet, and $p_T(\text{fast jet})$ for the \cancel{E}_T event sample. We have illustrated this by scatter plots in Fig. 2 for the two signal cases and for the dominant backgrounds. We see that by further requiring,

- (*v*) $p_T(\text{fast jet}) > 80$ GeV for $\Delta\phi > 90^\circ$; else $p_T(\text{fast jet}) > 50$ GeV,

we are able to substantially reduce the main SM backgrounds, with relatively modest loss of signal (particularly for the $\tilde{t}_1(125$ GeV) case, where the signal was indeed small compared to the backgrounds).

The resulting cross section from $\tilde{t}_1\tilde{t}_1^*$ production at the Tevatron, after cuts (*i-v*), is illustrated by the contour plot in the $m_{\tilde{t}_1}$ vs. $m_{\tilde{Z}_1}$ plane in Fig. 3. Also shown are the SM backgrounds after these same cuts. We note that although for certain regions of this parameter plane the chargino decay mode of the stop will necessarily be kinematically open *within the MSSM framework*, for the purposes of this figure, we have assumed that the charginos are too heavy to be produced via decays of the stops, and used the *FORCE* command in ISAJET to decay the stop via $\tilde{t}_1 \rightarrow c\tilde{Z}_1$. We terminate the contours for stop masses where the three body decay $\tilde{t}_1 \rightarrow bW\tilde{Z}_1$ becomes accessible, since then, the branching fraction for the two body mode $c\tilde{Z}_1$ mode is no longer unity. Several features of Fig. 3 are worth noting.

1. We see that the signal cross section after all cuts exceeds 1 pb for $m_{\tilde{t}_1}$ as large as $\sim 100 - 120$ GeV even if \tilde{Z}_1 is as heavy as 50 GeV. For this cross section contour, as many as 40 stop events may already be present in the accumulated data sample of the Tevatron.
2. The dominant SM background source is $W \rightarrow \tau\nu$ production, where the hadronically decaying τ is counted as one of the jets. Since τ jets almost always have a charged multiplicity of 1 or 3, it should be possible to discriminate the bulk of these events from the signal by vetoing low charged multiplicity jets. We show this background to allow the reader to assess the τ -jet discrimination factor which is necessary for

sufficient background rejection. If a rejection 80% of $W \rightarrow \tau$ events is achieved without substantial loss of signal, the stop signal exceeds combined background for $m_{\tilde{t}_1} \lesssim 100$ GeV, and $m_{\tilde{Z}_1} < 30 - 40$ GeV.

3. We note that the $Z \rightarrow \nu\bar{\nu}$ background can be reliably subtracted if a large enough data sample is accumulated for directly measuring high p_T Z bosons decaying to leptons, and using the Z branching ratios measured at LEP.
4. Unlike as in Ref. [15], where it was concluded that the stop signal was very small for $m_{\tilde{Z}_1} \gtrsim 20$ GeV, we see that the signal is quite robust even if \tilde{Z}_1 is heavy. In fact, we have checked that there is a significant signal level even if \tilde{Z}_1 is nearly degenerate with \tilde{t}_1 — for instance, for $m_{\tilde{t}_1} = m_{\tilde{Z}_1} + 5$ GeV = 105 GeV, the cross section after all cuts is 0.25 pb, which is more than 2% of the total stop production cross section of 11 pb. The sharp fall-off of the cross section with increasing $m_{\tilde{Z}_1}$ in the earlier parton level simulation occurred because the daughter charm quarks rapidly became too soft to satisfy the jet requirements. In the more realistic ISAJET simulation, the stop pair can be produced with a substantial p_T since it can recoil against jets from QCD radiation. For $m_{\tilde{t}_1} \simeq m_{\tilde{Z}_1}$, the stops give most of their momentum to the heavy \tilde{Z}_1 , so that $\cancel{E}_T \simeq p_T(\tilde{t}_1\tilde{t}_1)$ and the jets come from QCD radiation as, for instance, in the $Z \rightarrow \nu\bar{\nu}$ background.
5. If, as anticipated, the Tevatron experiments accumulate around 100 pb⁻¹ of integrated luminosity by the current run, we may anticipate at least 50 or more signal events in the data for $m_{\tilde{t}_1} \lesssim 100$ GeV even if \tilde{Z}_1 is relatively heavy. Although the background level, as read off from Fig. 3, would be around 200 events (assuming a $W \rightarrow \tau$ rejection of 80%), we should keep in mind that the actual background, after $Z \rightarrow \nu\bar{\nu}$ events are subtracted, will be considerably smaller. A several standard deviation signal should be possible for stops as heavy as 100-125 GeV. A precise evaluation of the Tevatron reach, which should take into account detector-dependent backgrounds, is beyond the scope of this study.

Up to this point, we have made no use of the fact that the signal always contains c -quark jets. It is clear that SM backgrounds would be considerably reduced if it were to be possible to tag at least one of the c -quarks. This led us to consider the possibility of using a muon from the semi-leptonic decay of one of the c quarks as a tag. The signal would then consist of $\mu + (n_j \geq 2) + (\cancel{E}_T \geq 50 \text{ GeV})$, where the muon is *within* a cone of $\Delta R = 0.4$ about one of the jets. For these muon-tagged events we require, in addition to (*i-iv*) above, that

- $p_T(\mu) \geq 3$ GeV for the muon to be identifiable, and
- either $\Delta\phi(j_{near}, \vec{\cancel{E}}_T) \leq 90^\circ$ or $p_T(j_{fast}) \geq 50$ GeV.

The signal cross section contours, with these cuts, are shown in Fig. 4 together with estimates of backgrounds from $W \rightarrow \tau\nu \rightarrow \mu\nu\nu\nu$, $W \rightarrow \mu\nu$ and $Z \rightarrow \nu\bar{\nu} + c\bar{c}$ or $b\bar{b}$ processes. To estimate these, we have generated 14K (130K) W (Z) events of each type, and find that just 8, 5 and 6 events, respectively, pass our cuts. It should also be kept in mind that ISAJET does not include the full 2 \rightarrow 3 matrix elements for $Zc\bar{c}$ or $Zb\bar{b}$ production; in our

simulation, these events come from radiation of initial state gluons followed by splitting into $b\bar{b}$ or $c\bar{c}$ pairs.

We see from Fig. 4 that even with an integrated luminosity of 100 pb^{-1} , there will be only 5-10 tagged events for sparticle masses such that the \cancel{E}_T signal shown in Fig. 3 might be difficult to observe above the background. We further see that the 0.2 pb contour in Fig. 4 (which roughly maps out the region where $S/B \geq 1$) essentially tracks the contour where the \cancel{E}_T signal in Fig. 3 equals the $Z \rightarrow \nu\bar{\nu}$ background. We thus conclude that the use of muon tagging does not extend the reach of the Tevatron to discover stop squarks in the \cancel{E}_T channel. Nevertheless, observation of μ -tagged \cancel{E}_T events could be important, even at low rates: non-observation of these events at expected rates would rule out a $\tilde{t}_1 \rightarrow c\tilde{Z}_1$ decay hypothesis.

IV. SEARCH FOR STOPS DECAYING TO CHARGINOS PLUS BOTTOM

If $m_{\tilde{t}_1} > m_{\tilde{W}_1} + m_b$, the stop decays via the two-body chargino mode with a branching fraction of nearly 100%. Charginos with $m_{\tilde{W}_1} \lesssim 100\text{ GeV}$ typically decay via the three-body mode $\tilde{W}_1 \rightarrow f\bar{f}'\tilde{Z}_1$ ($f = q$ or ℓ) mediated by a virtual W , \tilde{q}_L or $\tilde{\ell}_L$. Since sfermion masses are likely to be larger than M_W , the W^* mediated decays dominate over large ranges of SUSY parameters, so that the branching fractions for chargino decays are, generally speaking, close to those of the W -boson. It is only when the lightest neutralino is dominantly a $U(1)$ gaugino that the $W\tilde{W}_1\tilde{Z}_1$ coupling is dynamically suppressed; then the sfermion-mediated amplitudes become especially important. If, in addition, sleptons are also considerably lighter than squarks as is the case in the no scale limit of supergravity models, the branching fractions for chargino leptonic decays can be significantly enhanced. Here, we have mainly confined our attention to the more typical case where W^* -mediated decays indeed dominate. It is, however, worth remembering that the leptonic signals discussed here may be enhanced in some regions of parameter space.

If both the charginos in a stop pair production event decay hadronically, the signal is qualitatively the same as that in Sec. III: *i.e.*, consisting of $n - jet + \cancel{E}_T$ events. Since, in the present case, the \tilde{Z}_1 is always produced via a two-step cascade, we expect [7] that the \cancel{E}_T spectrum would be softer than that shown in Fig. 1, so that SM backgrounds to the signal could be problematic. For this reason, we focus on the signal where one (or both) of the charginos decay leptonically. This stop signal, which consists of events with 1 or 2 isolated leptons together with jet(s) and \cancel{E}_T (from the undetected \tilde{Z}_1 's and neutrino(s)), has the same event topology as the canonical signal for top quarks. It is, therefore, essential to devise strategies to separate the stop signal events from top background, keeping in mind that cuts designed to optimize the top quark signal may not be suitable for the detection of \tilde{t}_1 squarks [15].

A. The Single Lepton Signal.

At the Tevatron, single lepton events from the cascade decays of gluinos and squarks are expected [7] to be swamped by backgrounds from high p_T W production, with the isolated lepton coming from the decay of the W . What is different about stop events is that each

event contains two hard, central b -quark jets which may be tagged using a silicon microvertex detector. In our computation, we assume [19] 40% of the events have the vertex within the SVX barrel. For these events, we take the efficiency for detecting B -hadrons with $p_T > 15$ GeV and $|\eta_B| < 1$ to be 30%. In our analysis of the 1ℓ signal, we have required the following:

- (i) one isolated e (μ) with $p_T > 10$ GeV (5 GeV),
- (ii) two or more jets with at least one of the jets in the central region $|\eta_j| < 2$,
- (iii) $\cancel{E}_T > 25$ GeV, and
- (iv) at least one tagged B -hadron.

The main SM backgrounds to the single lepton signal come from $W \rightarrow \ell\nu + jet$ production, and from $t\bar{t}$ production and are shown in Table I for $m_t = 140$ GeV and $m_t = 170$ GeV along with the signal with $m_{\tilde{t}_1} = 100$ GeV, $m_{\tilde{W}_1} = 70$ GeV and $m_{\tilde{Z}_1} = 30$ GeV. We emphasize that b -tagging capability as assumed above is absolutely essential for the identification of the signal above the W background. ISAJET generates $Wb\bar{b}$ events from initial state gluon radiation followed by gluon splitting, using the usual collinear QCD matrix elements of the parton shower model. We have checked that without the b -tagging requirement (iv), the signal to W background ratio would be degraded by a factor > 250 .

We see from Table I that the stop signal is considerably smaller than the total SM background. We have studied distributions that may serve to enhance the signal-to-background ratio. The multiplicity distribution of jets in the stop signal (solid) and in the top background for $m_t = 140$ GeV (dotted) and $m_t = 170$ GeV (dashed-dotted), after cuts (i-iv) is shown in Fig. 5a. We have illustrated the signal for $m_{\tilde{t}_1} = 100$ GeV, $m_{\tilde{W}_1} = 70$ GeV, and $m_{\tilde{Z}_1} = 30$ GeV. As expected, the top background has a significantly larger jet multiplicity than the signal. We have checked that this is true even if \tilde{t}_1 is as heavy as 130 GeV. To enhance the stop signal to top background ratio *without much loss of signal*, we have required

- (v) $n_{jet} \leq 4$.

In this choice we have been guided by the fact that the number of signal events in the data sample of the *current* Tevatron run, which is expected to accumulate an integrated luminosity of $100 pb^{-1}$, is not very large. It is clear, however, that if a significantly larger data sample is available (as should be possible after the main injector upgrade), choosing $n_{jet} \leq 3$ (recall we always require at least two jets in the signal) optimizes the stop signal to top background ratio.

The signal-to-background ratio can be further improved by recognizing that in both the top and W backgrounds the lepton and much of the \cancel{E}_T come from the decay of a single W -boson. We thus expect that the transverse mass distribution $d\sigma/dm_T(\ell, \cancel{E}_T)$ for the background exhibits a characteristic Jacobian peak while the signal should show no such feature. Toward this end, we show this distribution, after cuts (i-v) in Fig. 5b for the same signal case as in Fig. 5a (solid), the $W \rightarrow \ell\nu$ background (dashes) and the $t\bar{t}$ background for $m_t = 140$ GeV (dotted). The transverse mass distribution will thus exhibit substantial distortion for low $m_T(\ell, \cancel{E}_T)$ if a signal is present. We see that by further requiring,

- (vi) $m_T(\ell, \cancel{E}_T) \leq 45$ GeV,

we are able to eliminate a large fraction of the background with a relatively modest loss of signal. The background, including cuts (v) and (vi), is shown in the last column in Table I. We see that a signal-to-background ratio of unity is possible for $m_{\tilde{t}_1} < 100$ GeV, even for the unfavourable $m_t = 140$ GeV case. Finally, we examined whether tails from direct $b\bar{b}$ production, which has an enormous cross section at the Tevatron, could possibly fake the stop signal. We simulated 3M $b\bar{b}$ events, and found that only one event passes our cuts. Applying the b -tagging efficiency, we estimate that this background to be ~ 24 fb, with large errors.

In Fig. 6, we show contours of constant cross section for the single lepton signal in the $m_{\tilde{t}_1}$ vs. $m_{\tilde{W}_1}$ plane for $\mu = -m_{\tilde{g}}$ and $\tan\beta = 2$. The corresponding \tilde{Z}_1 mass is also shown on the right. We have cut off the contours for $m_{\tilde{Z}_1} < 20$ GeV since this region is excluded [20] within the MSSM framework. We see that unlike Fig. 3, where the cross section remains substantial even for \tilde{Z}_1 masses close to $m_{\tilde{t}_1}$, the single lepton signal rapidly decreases when $m_{\tilde{t}_1}$ approaches $m_{\tilde{W}_1}$. This is because the b -jet becomes very soft and so is not tagged. We also see that $\gtrsim 20$ signal events (compared to a background of 6-11 events, depending on m_t) may be expected in a Tevatron data sample of 100 pb $^{-1}$ for $m_{\tilde{t}_1} < 90$ GeV if $m_{\tilde{W}_1} \lesssim 60$ GeV. This corresponds to about a 6σ effect in the data sample expected to be accumulated by the end of the current Tevatron run, *provided that sufficient b -tagging efficiency is achieved*. In the longer term, the Tevatron may be able to probe a stop mass in excess of 100 GeV in this channel, particularly after the main injector becomes operational.

B. The Dilepton Signal.

Finally, we consider the dilepton signal arising from $\tilde{t}_1\tilde{t}_1^{\bar{}}$ events where both the charginos decay leptonically. For this signal, we require:

- (i) *at least* two unlike sign, isolated leptons (e or μ), with $p_T(e) > 8$ GeV and $p_T(\mu) > 5$ GeV,
- (ii) $20^\circ < \Delta\phi(\ell^+, \ell'^-) < 160^\circ$ (to reduce Drell-Yan background),
- (iii) at least one jet with $|\eta_j| < 2$,
- (iv) $\cancel{E}_T > 25$ GeV.

The SM backgrounds to this signal, which dominantly come from $t\bar{t}$ production and W pair production, are shown in Table II after the cuts (i-iv). Also shown is the bound on this cross section we get from a simulation of 10M $b\bar{b}$ events, none of which pass our cuts. For comparison, we also show the signal for the same case as in Table I. We see that the signal is smaller than the SM backgrounds even for the heavier top case. Unlike the case for the single lepton signal, there is no obvious kinematic variable like the transverse mass that can be used to enhance the signal relative to the background. We note, however, that the leptons from the three-body chargino decays are expected to be softer than background, which has two-body decays of real W bosons.

With this in mind, we examined several distributions (to be discussed shortly) that may help to distinguish the top squark signal from the SM backgrounds. We found that the distribution of the scalar sum of the transverse momenta of the two leptons plus the \cancel{E}_T in each event, which we refer to as “bigness”, or B ,

$$B = |p_T(\ell^+)| + |p_T(\ell^-)| + |\cancel{E}_T|, \quad (8)$$

provides optimal distinction between the signal and the (dominant) top quark background. This distribution is shown in Fig. 7a for the signal from a 100 GeV stop decaying into a chargino (solid) and for the $t\bar{t}$ background for $m_t = 140$ GeV. As anticipated, the distribution is considerably harder for the background than for the signal; requiring

- (v) $B < 100$ GeV,

in addition to cuts ($i-v$), significantly improves the signal to background ratio. The SM backgrounds, including this cut, are shown in the last column of Table II. The difference in the signal and background “bigness” distributions is illustrated in an alternative fashion in Fig. 7b, where we have shown on the horizontal (vertical) axis the signal (top background) cross section integrated up to the value of B marked on the curve in this figure. In other words, the signal (background) cross section is 80 fb (15 fb) if $B < 80$ GeV. It is clear that the best distributions for distinguishing the signal from background are those where the slope of the corresponding curve remains small for a large distance after which it turns upward. Furthermore, since we can read off the value of B for any point along the curve, Fig. 7b enables us to easily find an optimal value for the cut. We see that $B < 100$ GeV that we obtained from the histogram in Fig. 7a is indeed a good choice for the cut.

In Fig. 8, we have shown the analogous curves for other combinations of the lepton momenta and \cancel{E}_T that may serve to distinguish the signal from background for the same cases as in Fig. 7. We show (a) the bigness distribution (again, for ease of comparison), (b) the \cancel{E}_T distribution, (c) the distribution of the scalar sum, $|p_T(\ell^+)| + |p_T(\ell^-)|$, and (d) the p_T distribution of the hard lepton. From the shapes of these curves, it should be clear that the “bigness” distribution is indeed the best one to distinguish between stop and top production.

We have illustrated the p_T distributions of the two leptons in the dilepton signal as well as the corresponding \cancel{E}_T distributions, after cuts ($i-v$), in Fig. 9 for (a) $m_{\tilde{t}_1} = 100$ GeV, $m_{\tilde{W}_1} = 90$ GeV and $m_{\tilde{Z}_1} = 42$ GeV, (b) $m_{\tilde{t}_1} = 100$ GeV, $m_{\tilde{W}_1} = 60$ GeV and $m_{\tilde{Z}_1} = 23$ GeV, and (c) $m_{\tilde{t}_1} = 70$ GeV, $m_{\tilde{W}_1} = 60$ GeV and $m_{\tilde{Z}_1} = 23$ GeV. The fast lepton and \cancel{E}_T distributions in cases (a) and (b) are considerably harder than in case (c) where the stop is rather light and $m_{\tilde{W}_1} - m_{\tilde{Z}_1}$ is small. Also, for a given value of $m_{\tilde{t}_1}$, these distributions become softer with decreasing difference between the chargino and the LSP mass. The slow lepton p_T distributions are, however, backed up against the cut. These distributions also enable the reader to assess the effect on the signal if the cut on the lepton p_T is further relaxed. Clearly, capability for detection of leptons near the edge of the $p_T(\ell)$ cut (i) in events triggered by jets and/or \cancel{E}_T is required in order not to lose too much of the signal.

In Fig. 10, we show the cross section contours for the dilepton signal after all the cuts for $m_{\tilde{g}} = -\mu$, and $\tan\beta = 2$ in the $m_{\tilde{t}_1} - m_{\tilde{W}_1}$ plane. The region below the horizontal dashed line is experimentally excluded [20] within the MSSM framework, while in the region above the sloping dashed line, the stop decays via the flavour-changing loop decay mode analysed

in Sec. III. We see that while the signal is rather small, it exceeds the SM backgrounds for $m_{\tilde{t}_1} < 110$ GeV (130 GeV) for $m_t = 140$ GeV (170 GeV) even if \tilde{Z}_1 is heavy. In a data sample with an integrated luminosity of 100 pb^{-1} that should be accumulated by the end of the current Tevatron run, we may expect > 10 signal events compared to a background of 3-6 events, depending on the top quark mass, if $m_{\tilde{t}_1} < 100$ GeV. Thus the Tevatron experiments should soon be able to probe top squark masses up to just under 100 GeV (larger, if the top is discovered and found to be heavy) even in the dilepton channel. This should increase to 120-130 GeV after the main injector becomes operational and the top turns out to be heavy. We remark that unlike as for the single lepton signal, the detection of the signal in the dilepton channel does not rely on the capability for tagging displaced vertices.

We remind the reader that in all our computations up to this point, we have chosen parameters so that the leptonic branching fraction for chargino decays is 11% per lepton family. As mentioned above, this may be considerably enhanced [21] if sleptons are lighter than squarks and the \tilde{Z}_1 is mainly a U(1) gaugino. For instance, for $m_{\tilde{q}} = m_{\tilde{g}} = 250$ GeV, $\mu = -400$ GeV with $\tan \beta = 20$ (which yields $m_{\tilde{W}_1} = 70$ GeV, $m_{\tilde{Z}_1} = 35$ GeV and slepton masses around 125 GeV), this branching fraction increases to about 30%. For this case, we find the b -tagged single-lepton (dilepton) cross section after all cuts of 220 fb (780 fb) for a stop mass of 100 GeV to be compared with 140 fb (130 fb) in Table I. Our point here is to illustrate that the leptonic cross sections can indeed be significantly enhanced for reasonable choices of SUSY parameters, and that these enhancements are in keeping with expectations from the increase in the leptonic branching fraction of the chargino. In such scenarios, it may be possible to probe stop masses significantly beyond 100 GeV by the end of Run I B of the Tevatron. To illustrate, we have checked that for $m_{\tilde{t}_1} = 130$ GeV, the choice $m_{\tilde{q}} = m_{\tilde{g}} = 315$ GeV, $\mu = -500$ GeV and $\tan \beta = 20$, yields cross sections of 63 fb and 210 fb in the single-lepton and dilepton channels, respectively. It is amusing to see that the dilepton signal can be considerably larger than the signal in the single-lepton channel.

V. DISCUSSION AND CONCLUSIONS

We have seen that, in the framework of supergravity models, the lighter of the two top squarks (\tilde{t}_1) may be very light even if the other squarks and gluinos have masses of several hundred GeV. Current Tevatron experimental analyses [5,6] on squark masses are not applicable to a single light top squark, so that currently the best limit is still $m_{\tilde{t}_1} \gtrsim 45$ GeV, based on non-observation of a signal at LEP. Hence, one of most favorable routes towards the discovery of supersymmetry at the Fermilab Tevatron collider may be to search for the light top squark. We have shown in this paper that Tevatron experiments ought to be able to explore top squark masses of ~ 100 GeV, given an integrated luminosity of $\sim 100 \text{ pb}^{-1}$. Thus, Tevatron collider experiments ought to be able to either discover supersymmetry via the top squark, or place an important new limit on its mass. Such a limit can serve to constrain the GUT scale parameter space of supergravity models, where the \tilde{t}_1 mass is driven to small values by a large top quark Yukawa coupling. In fact, model builders already have to take care to ensure that $m_{\tilde{t}_1}^2$ is not driven negative, leading to breaking of electromagnetic and colour gauge symmetries [1].

If $m_{\tilde{t}_1} < m_b + m_{\tilde{W}_1}$, then $\tilde{t}_1 \rightarrow c\tilde{Z}_1$, so collider experiments ought to search for $p\bar{p} \rightarrow \tilde{t}_1\tilde{t}_1 \rightarrow c\bar{c}\tilde{Z}_1\tilde{Z}_1$, leading to a multi-jet plus \cancel{E}_T signature. Even after suitable cuts, significant

backgrounds from W and Z production remain. The \cancel{E}_T signal cross section, which depends only on the \tilde{t}_1 and \tilde{Z}_1 masses, is conveniently summarized by cross section contours in the $m_{\tilde{t}_1} - m_{\tilde{Z}_1}$ plane in Figs. 3 and 4. Assuming that the backgrounds can indeed be reliably suppressed/subtracted out from the data sample (via τ -jet veto, Z +jets total normalization, *etc.*), we see that \tilde{t}_1 masses of $\sim 80-100$ GeV ought to be accessible to Tevatron experiments by the end of the current run.

If $m_{\tilde{t}_1} > m_b + m_{\tilde{W}_1}$, then $\tilde{t}_1 \rightarrow b\tilde{W}_1$, so collider experiments ought to search for $p\bar{p} \rightarrow \tilde{t}_1\tilde{t}_1 \rightarrow b\bar{b}\tilde{W}_1\tilde{W}_1$, where $\tilde{W}_1 \rightarrow \ell\nu\tilde{Z}_1$ or $q\bar{q}'\tilde{Z}_1$. Just as for the top quark search, signals appear most promising in the single and dilepton final states. For single lepton final states, B -tagging capability is essential to veto the large W +multi-jet background. The results of our computation of the single-lepton and the dilepton signal are summarized in Fig. 6 and Fig. 10, respectively. Given sufficient B -tagging capability, \tilde{t}_1 masses to 80-100 GeV ought to be explorable at the Tevatron via the single lepton channel. For the dilepton signal, major backgrounds come from $t\bar{t}$ and WW production. Requiring “soft” dilepton events, (*e.g.*, requiring $B = |p_T(\ell_1)| + |p_T(\ell_2)| + \cancel{E}_T < 100$ GeV), allows sufficient rejection of background that, as before, stop masses of ~ 100 GeV ought to be probed at the Tevatron by the end of the current run.

The analysis in the present paper is a conservative one, in that an additional source of stop squark production, $t \rightarrow \tilde{t}_1\tilde{Z}_1$, has been neglected. This decay mode, which can have branching fractions of up to $\sim 30\%$, would contribute an additional signal, as well as diminish the SM top quark background [15]. It would be interesting to investigate whether the observation of a top quark signal at a rate consistent with SM expectations could be used to independently constrain $m_{\tilde{t}_1}$ at a top factory. We have also been conservative in that for the leptonic signals from stop production shown in Figs. 6 and 10, we have chosen parameters so that the branching fractions for leptonic decays of charginos are essentially the same as those of the W boson; as discussed in the text, the single lepton (dilepton) signals may be enhanced by a factor of ~ 1.5 (~ 6) for certain ranges of SUSY parameters.

In summary, the search for stop squarks adds a new avenue to the search for supersymmetry at the Tevatron collider. Light top squarks have a significant degree of theoretical motivation. We have attempted to show in this paper that our experimental colleagues ought to be able either to discover top squarks at the Tevatron, or to significantly extend the limit on their mass.

ACKNOWLEDGMENTS

We thank S. Blessing, A. Boehnlein, A. Goshaw and A. White for discussions. This research was supported in part by the U. S. Department of Energy under contract number DE-FG05-87ER40319 and DE-AM03-76SF00235. In addition, the work of HB was supported by the TNRLC SSC Fellowship program.

REFERENCES

- [1] For reviews of supersymmetry phenomenology, see H. P. Nilles, Phys. Rep. **110**, 1 (1984); P.Nath, R.Arnowitz and A. Chamseddine, *Applied N = 1 Supergravity*, ICTP Series in Theoretical Physics, Vol.I, World Scientific (1984); H. Haber and G. Kane, Phys. Rep. **117**, 75 (1985); X. Tata, in *The Standard Model and Beyond*, p. 304, edited by J. E. Kim, World Scientific (1991); V. Barger and R. J. N. Phillips, Wisconsin preprint, MAD/PH/765; R. Arnowitt and P. Nath, *Lectures presented at the VII J.A. Swieca Summer School, Campos do Jordao, Brazil, 1993* CTP-TAMU-52/93.
- [2] U. Amaldi, W. de Boer and H. Furstenau, Phys. Lett. **B260**, 447 (1991); J. Ellis, S Kelley and D. Nanopoulos, Phys. Lett. **B260**, 131 (1991); P. Langacker and M. Luo, Phys. Rev. **D44**, 817 (1991).
- [3] Some recent analyses of supergravity mass spectra include, G. Ross and R. G. Roberts, Nucl. Phys. **B377**, 571 (1992); R. Arnowitt and P. Nath, Phys. Rev. Lett. **69**, 725 (1992); M. Drees and M. M. Nojiri, Nucl. Phys. **B369**, 54 (1993); S. Kelley *et. al.* Nucl. Phys. **B398**, 3 (1993); D. Castano, E. Piard and P. Ramond, UFIFT-HEP-93-18 (1993); G. Kane, C. Kolda, L. Roszkowski and J. Wells, UM-TH-93-24 (1993); V. Barger, M. Berger and P. Ohmann, MAD/PH/801 (1993).
- [4] H. Baer, C. Kao and X. Tata, Phys. Rev. **D48**, 2978 (1993); T. Tsukamoto, K. Fujii, H. Murayama, M. Yamaguchi and Y. Okada, KEK preprint 93-146; J. Lopez, D. Nanopoulos, G. Park, X. Wang and A. Zichichi, CERN preprint, CERN-TH 7139/94 (1993); H. Baer, M. Drees, C. Kao, M. Nojiri and X. Tata, Florida State University preprint FSU-HEP-940311 (1994).
- [5] F. Abe *et. al.* Phys. Rev. Lett. **69**, 3439 (1992).
- [6] A. White, presented at the Aspen Winter Conference on Particle Physics, Aspen, CO (1994).
- [7] H. Baer, X. Tata and J. Woodside, Phys. Rev. **D44**, 207 (1992).
- [8] K. Inoue, A. Kakuto, H. Komatsu and H. Takeshita, Prog. Theor. Phys. **68**, 927 (1982) and **71**, 413 (1984); L. Ibanez and C. Lopez, Nucl. Phys. **B233**, 511 (1984).
- [9] J. Ellis and S. Rudaz, Phys. Lett. **128B**, 248 (1983)
- [10] See *e.g.* A. Bouquet, J. Kaplan and C. A. Savoy, Nucl. Phys. **B262**, 299 (1985).
- [11] See M. Drees and M. Nojiri, Ref. [3].
- [12] D. Decamp *et.al.* (ALEPH Collaboration), Phys. Lett. **B236**, 86 (1990); P. Abreu *et.al.* (DELPHI Collaboration), Phys. Lett. **B247**, 157 (1990); O. Adriani *et.al.* (L3 Collaboration), CERN-PPE-93-31 (1993); M. Akrawy *et.al.* (OPAL Collaboration), Phys. Lett **B240**, 261 (1990); for a review, see G. Giacomelli and P. Giacomelli, CERN-PPE/93-107 (1993).
- [13] We do not consider the possibility that the $Z\tilde{t}_1\tilde{t}_1^*$ coupling accidentally vanishes when stop mixing is incorporated. The OPAL collaboration has recently studied this case even with $m_{\tilde{t}_1} \simeq m_{LSP}$ and have excluded $m_{\tilde{t}_1} < 20$ GeV even when the LSP-stop mass difference is just 2.2 GeV; for larger mass differences, the bound on the stop is more restrictive. See talk by T. Kobayashi at the 22nd INS International Symposium on Physics with High Energy Colliders, Tokyo, March 1994.
- [14] K. Hikasa and M. Kobayashi, Phys. Rev. **D36**, 724 (1987).
- [15] H. Baer, M. Drees, J. Gunion, R. Godbole and X. Tata, Phys. Rev. **D44**, 725 (1991).

- [16] F. Paige and S. Protopopescu, in *Supercollider Physics*, p. 41, ed. D. Soper (World Scientific, 1986); H. Baer, F. Paige, S. Protopopescu and X. Tata, in *Proceedings of the Workshop on Physics at Current Accelerators and Supercolliders*, ed. J. Hewett, A. White and D. Zeppenfeld, (Argonne National Laboratory, 1993).
- [17] A preliminary analysis of the stop signal for the case where the stop decays via the flavour-changing charm mode, was presented by H. Baer, J. Sender and X. Tata in *Proceedings of the Workshop on Physics at Current Accelerators and the Supercollider*, ed. J. Hewett, A. White and D. Zeppenfeld, (World Scientific, 1993).
- [18] E. Eichten, I. Hinchliffe, K. Lane and C. Quigg, *Rev. Mod. Phys.* **56**, 759 (1984).
- [19] A. Goshaw, private communication.
- [20] L. Roszkowski, *Phys. Lett.* **B252**, 471 (1991); M. Drees and X. Tata, *Phys. Rev.* **D43**, 2971 (1991); K. Hidaka, *Phys. Rev.* **D44**, 927 (1991); see also Ref. [7].
- [21] In the case where the sneutrino is light enough so that the two-body decay $\widetilde{W}_1 \rightarrow \tilde{\nu}\ell$ is accessible, the signal will be greatly degraded since the daughter lepton will generally be soft. Thus, the enhancement we refer to obtains only when sleptons and sneutrinos are significantly heavier than charginos, but lighter than squarks.

TABLES

TABLE I. Cross sections in fb at the Tevatron after cuts described in the text for SM background to the B -tagged single lepton signal. Also shown is the signal cross section for a representative case near the edge of the Tevatron reach, where we have taken $m_{\tilde{t}_1} = 100$ GeV, $m_{\tilde{W}_1} = 70$ GeV and $m_{\tilde{Z}_1} = 30$ GeV. Results have summed over e and μ .

process	Cuts ($i-iv$)	cuts($i-vi$)
$W \rightarrow \ell\nu$	440	30
$t\bar{t}(140)$	450	81
$t\bar{t}(170)$	170	32
$b\bar{b}$	24	24
$\tilde{t}_1\tilde{t}_1(100)$	240	140

TABLE II. Cross sections in fb at the Tevatron after cuts described in the text for SM backgrounds to the dilepton signal from top squark production. Also shown is the signal cross section for the same case as in Table I. Results have summed over e and μ .

process	Cuts ($i-iv$)	cuts($i-v$)
W^+W^-	50	10
$t\bar{t}(140)$	360	54
$t\bar{t}(170)$	135	14
$b\bar{b}$	< 48	
$\tilde{t}_1\tilde{t}_1(100)$	180	130

FIGURES

FIG. 1. \cancel{E}_T distributions, before any cuts, from $\tilde{t}_1\tilde{t}_1^*$ production in $p\bar{p}$ collisions at $\sqrt{s} = 1.8$ TeV for two choices of stop and \tilde{Z}_1 masses. Here, the stop is assumed to decay via $\tilde{t}_1 \rightarrow c\tilde{Z}_1$. Also shown are SM background distributions from $Z \rightarrow \nu\bar{\nu}$ production (dotted), $W \rightarrow \tau\nu$ production (dashed) and $W \rightarrow \mu\nu$ production (dot-dashed).

FIG. 2. The scatter plot for \cancel{E}_T events in the $\Delta\phi(\cancel{E}_T, j_{near}) - p_T(j_{fast})$ plane after cuts (*i-iv*) in Sec. III of the text for the $\tilde{t}_1\tilde{t}_1^*$ signal at the Tevatron for (a) $m_{\tilde{t}_1} = 85$ GeV, $m_{\tilde{Z}_1} = 20$ GeV, (b) $m_{\tilde{t}_1} = 125$ GeV, $m_{\tilde{Z}_1} = 40$ GeV, and dominant SM backgrounds from (c) $W \rightarrow \tau\nu$ production, and (d) $Z \rightarrow \nu\bar{\nu}$ production.

FIG. 3. Cross section (in pb) contours for the \cancel{E}_T distributions, after cuts (*i-v*) in Sec. III of the text, from $\tilde{t}_1\tilde{t}_1^*$ production in $p\bar{p}$ collisions at $\sqrt{s} = 1.8$ TeV, assuming that the stops decay via $\tilde{t}_1 \rightarrow c\tilde{Z}_1$. Also shown are dominant backgrounds from SM processes. The $W \rightarrow \tau$ background will be smaller if it is possible to veto τ jets at some level. Also, it may be possible to subtract the $Z \rightarrow \nu\bar{\nu}$ background as discussed in the text.

FIG. 4. The same as Fig. 3 except that, in this figure, we require a non-isolated muon with $p_T(\mu) > 3$ GeV to tag the c -jet. Cuts are as described in Sec. III of the text.

FIG. 5. (a) The jet multiplicity distribution in B -tagged single lepton events from stop pair production at a $p\bar{p}$ collider at $\sqrt{s} = 1.8$ TeV, assuming that stop decays via $\tilde{t}_1 \rightarrow b\tilde{W}_1$ after cuts (*i-iv*) in Sec. IV.A of the text. We illustrate the distribution from the signal (solid) for $m_{\tilde{t}_1} = 100$ GeV, $m_{\tilde{W}_1} = 70$ GeV and $m_{\tilde{Z}_1} = 30$ GeV, and from top quark backgrounds for $m_t = 140$ GeV (dotted) and $m_t = 170$ GeV (dashed-dotted), and (b) the transverse mass $m_T(\ell, \cancel{E}_T)$ distribution in these events after cuts (*i-v*) in Sec. IV.A of the text. We illustrate the distribution from the signal (solid) for the same SUSY masses as in (a), and from the dominant SM backgrounds from $W \rightarrow \ell\nu$ production (dashed) and $t\bar{t}$ production for $m_t = 140$ GeV (dotted). The branching fraction for $\tilde{W}_1 \rightarrow e\nu\tilde{Z}_1$ decay is 11%. If the top quark has a mass of 170 GeV, its contribution to the background is significantly smaller.

FIG. 6. Cross section (in fb) contours in the $m_{\tilde{t}_1} - m_{\tilde{W}_1}$ plane for B -tagged single lepton events from stop pair production at a $p\bar{p}$ collider at $\sqrt{s} = 1.8$ TeV, assuming that stop decays via $\tilde{t}_1 \rightarrow b\tilde{W}_1$ after cuts (*i-vi*) in Sec. IV.A of the text. The branching fraction for $\tilde{W}_1 \rightarrow e\nu\tilde{Z}_1$ decay is 11%. Also shown are the main SM backgrounds. The mass of \tilde{Z}_1 is illustrated on the right.

FIG. 7. (a) Distributions of the “bigness” variable B defined in Sec. IV.B of the text for dilepton events from stop pair production at the Tevatron (where the stop decays via $\tilde{t}_1 \rightarrow b\tilde{W}_1$) and from the background from production of 140 GeV $t\bar{t}$ pairs after cuts (i - iv) in Sec. IV.B of the text. The sparticle masses and chargino branching fractions are as in Fig. 5. (b) The cross section for stop dilepton signal (top background) on the horizontal (vertical) axis, integrated up to the value of B on the curve after the same cuts as in (a). This plot is described in more detail in Sec. IV.B.

FIG. 8. Cross sections with (a) the bigness, (b) \cancel{E}_T , (c) $|p_T(\ell_1)| + |p_T(\ell_2)|$, and (d) $p_T(\ell_{fast})$ variables integrated up to the values shown on the respective curves, for stop dilepton events (horizontal axis) and $t\bar{t}$ background, for $m_t = 140$ GeV, after cuts (i - iv) of Sec. IV.B.

FIG. 9. Distributions of the transverse momentum of the two leptons in dilepton events from stop pair production at the Tevatron along with the \cancel{E}_T distribution after cuts (i - v) in Sec. IV.B for three illustrative cases of \tilde{t}_1 , \tilde{W}_1 and \tilde{Z}_1 masses mentioned in the text.

FIG. 10. Cross section (in fb) contours for the dilepton cross section from the production of stop pairs at a $p\bar{p}$ collider with $\sqrt{s} = 1.8$ TeV, including cuts (i - v) of Sec. IV.B. The branching fraction for $\tilde{W}_1 \rightarrow e\nu\tilde{Z}_1$ decay is 11%. Also shown are the main SM backgrounds.

This figure "fig1-1.png" is available in "png" format from:

<http://arxiv.org/ps/hep-ph/9404342v1>

This figure "fig1-2.png" is available in "png" format from:

<http://arxiv.org/ps/hep-ph/9404342v1>

This figure "fig1-3.png" is available in "png" format from:

<http://arxiv.org/ps/hep-ph/9404342v1>

This figure "fig1-4.png" is available in "png" format from:

<http://arxiv.org/ps/hep-ph/9404342v1>

This figure "fig1-5.png" is available in "png" format from:

<http://arxiv.org/ps/hep-ph/9404342v1>

This figure "fig1-6.png" is available in "png" format from:

<http://arxiv.org/ps/hep-ph/9404342v1>

This figure "fig1-7.png" is available in "png" format from:

<http://arxiv.org/ps/hep-ph/9404342v1>

This figure "fig1-8.png" is available in "png" format from:

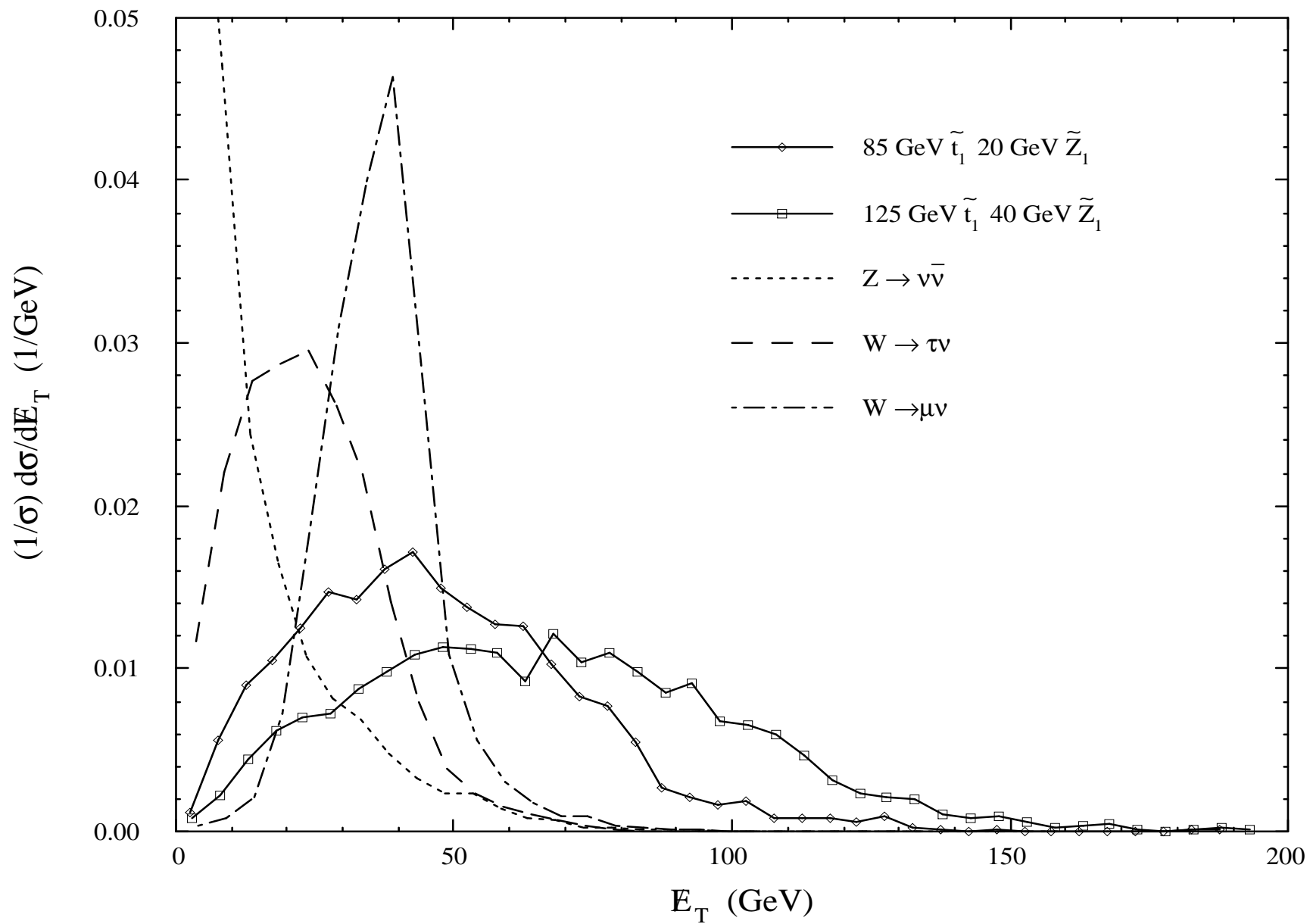
<http://arxiv.org/ps/hep-ph/9404342v1>

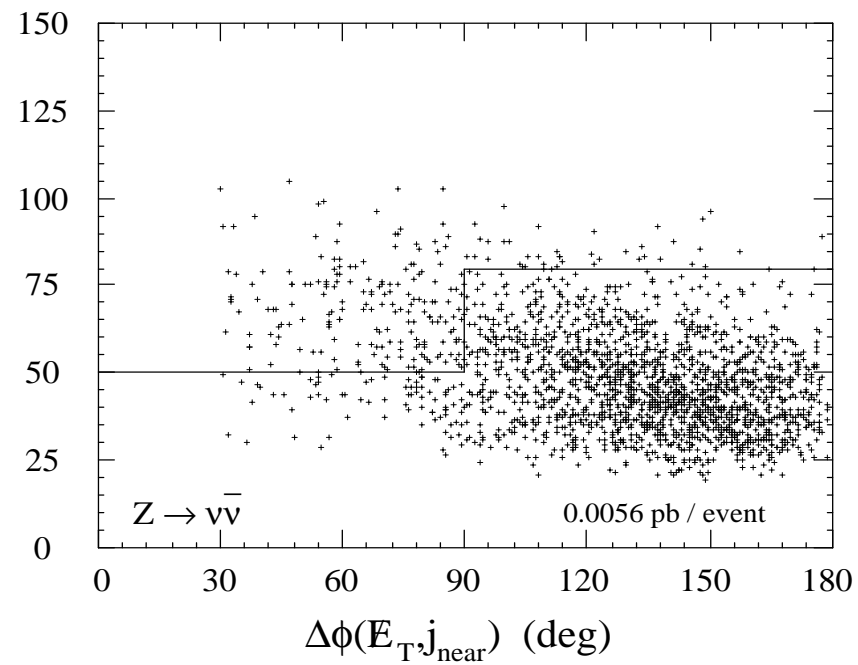
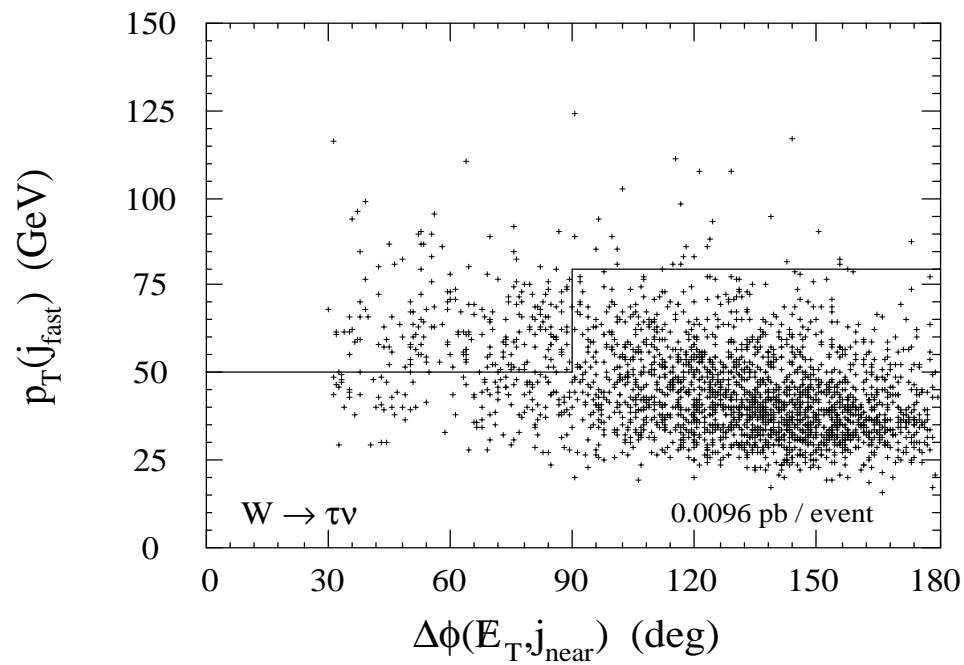
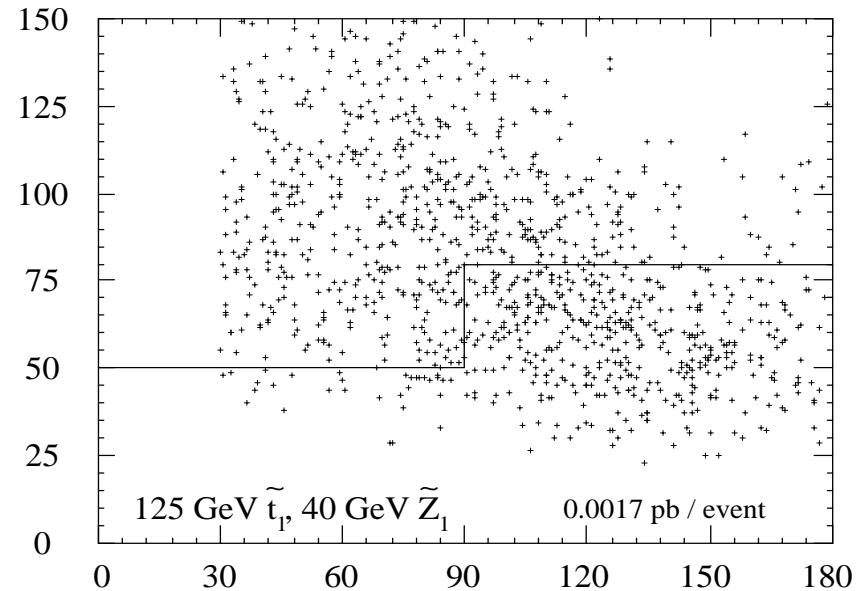
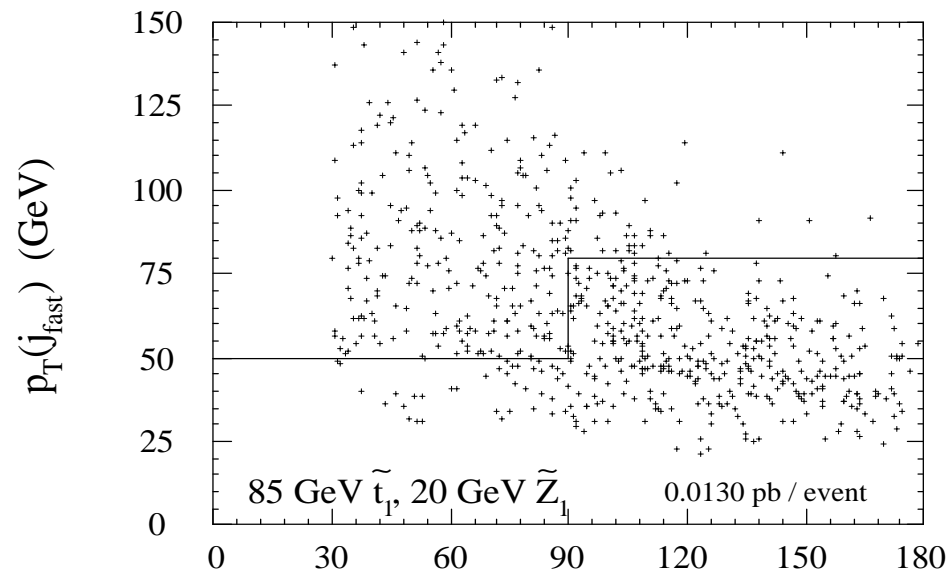
This figure "fig1-9.png" is available in "png" format from:

<http://arxiv.org/ps/hep-ph/9404342v1>

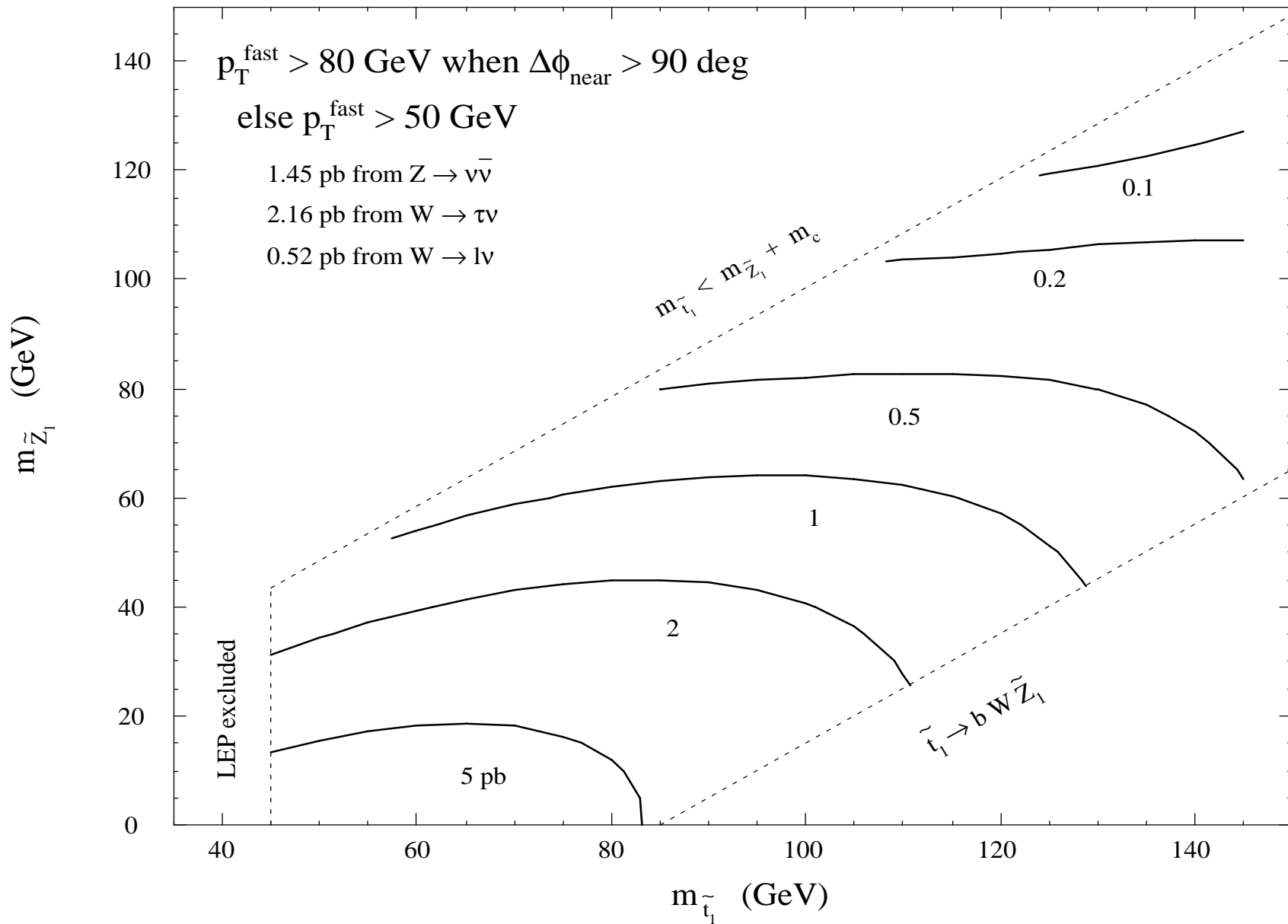
This figure "fig1-10.png" is available in "png" format from:

<http://arxiv.org/ps/hep-ph/9404342v1>

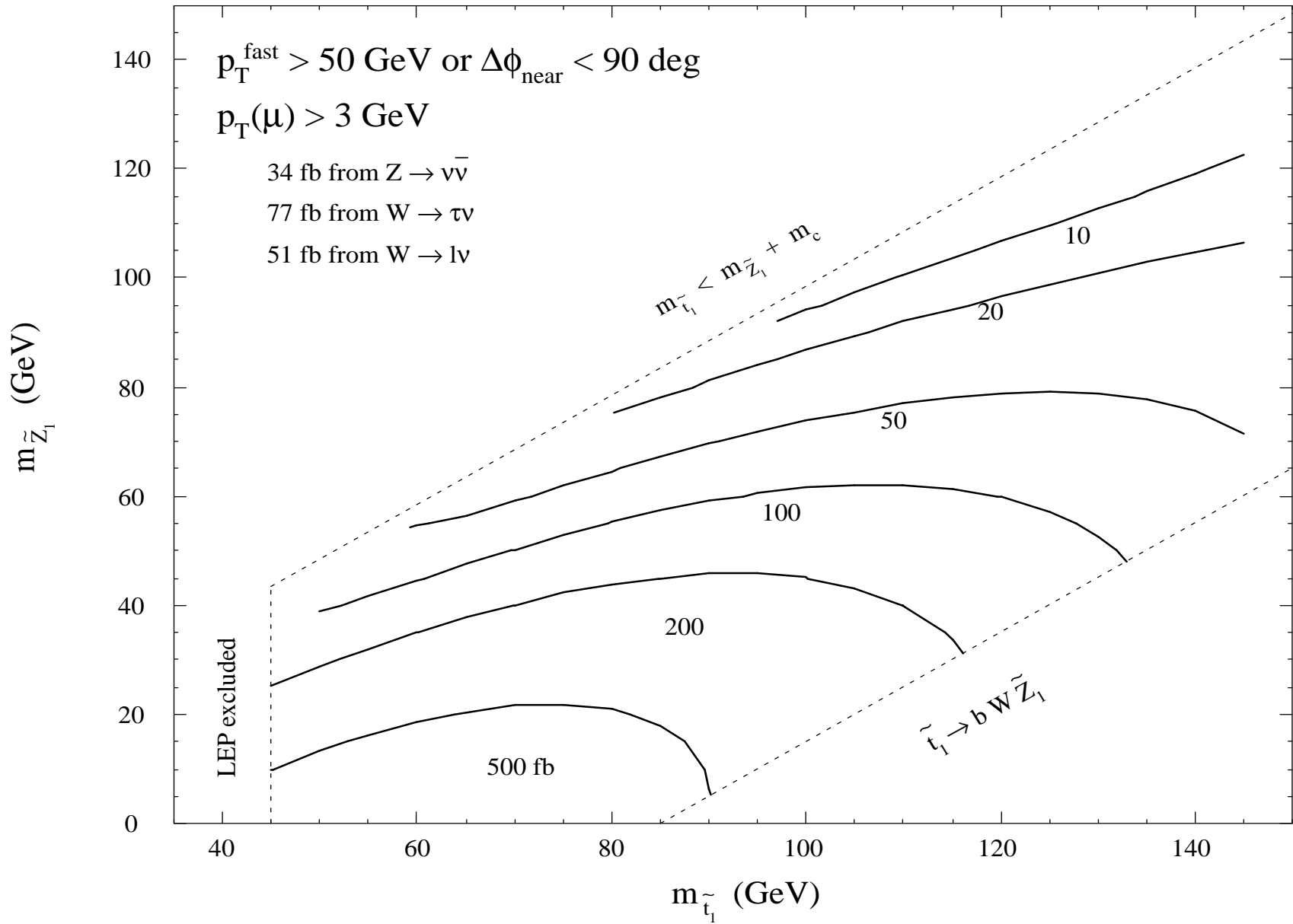


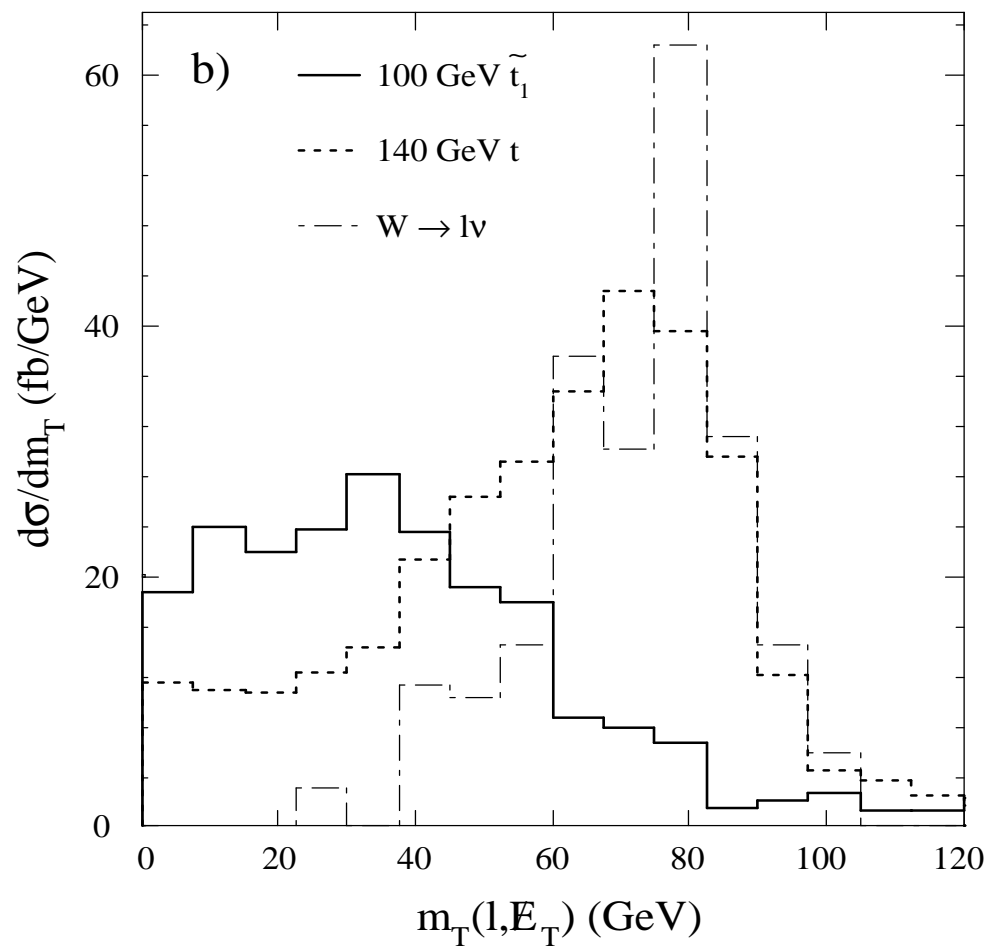
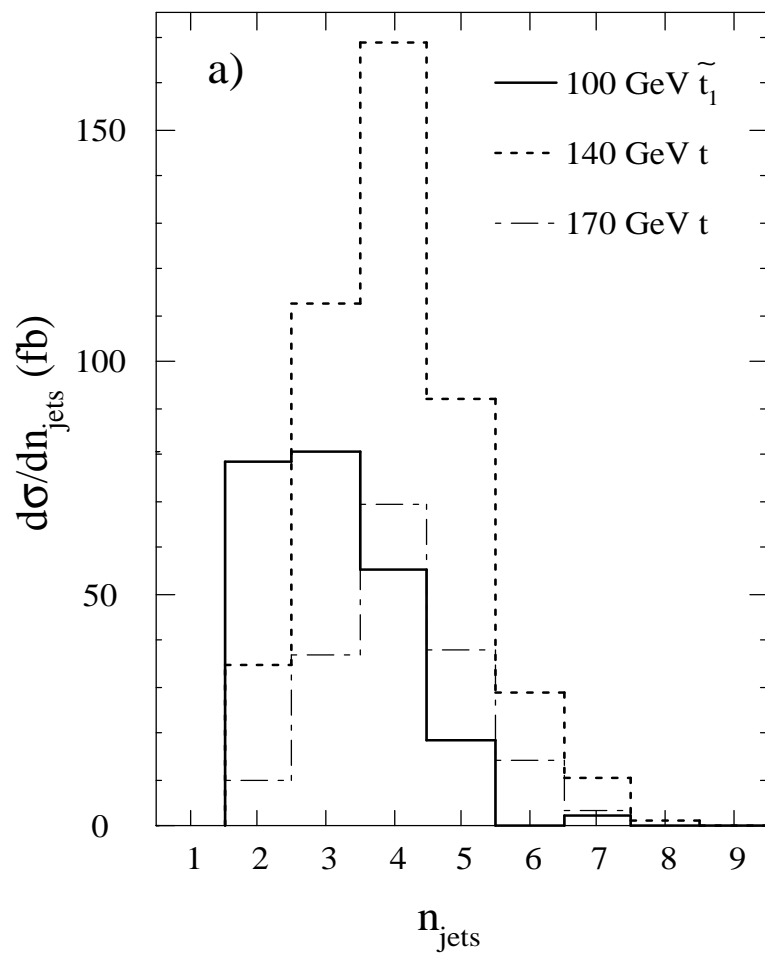


$E_T + \text{jets}$ cross section for $\tilde{t}_1 \rightarrow c \tilde{Z}_1$ (pb)

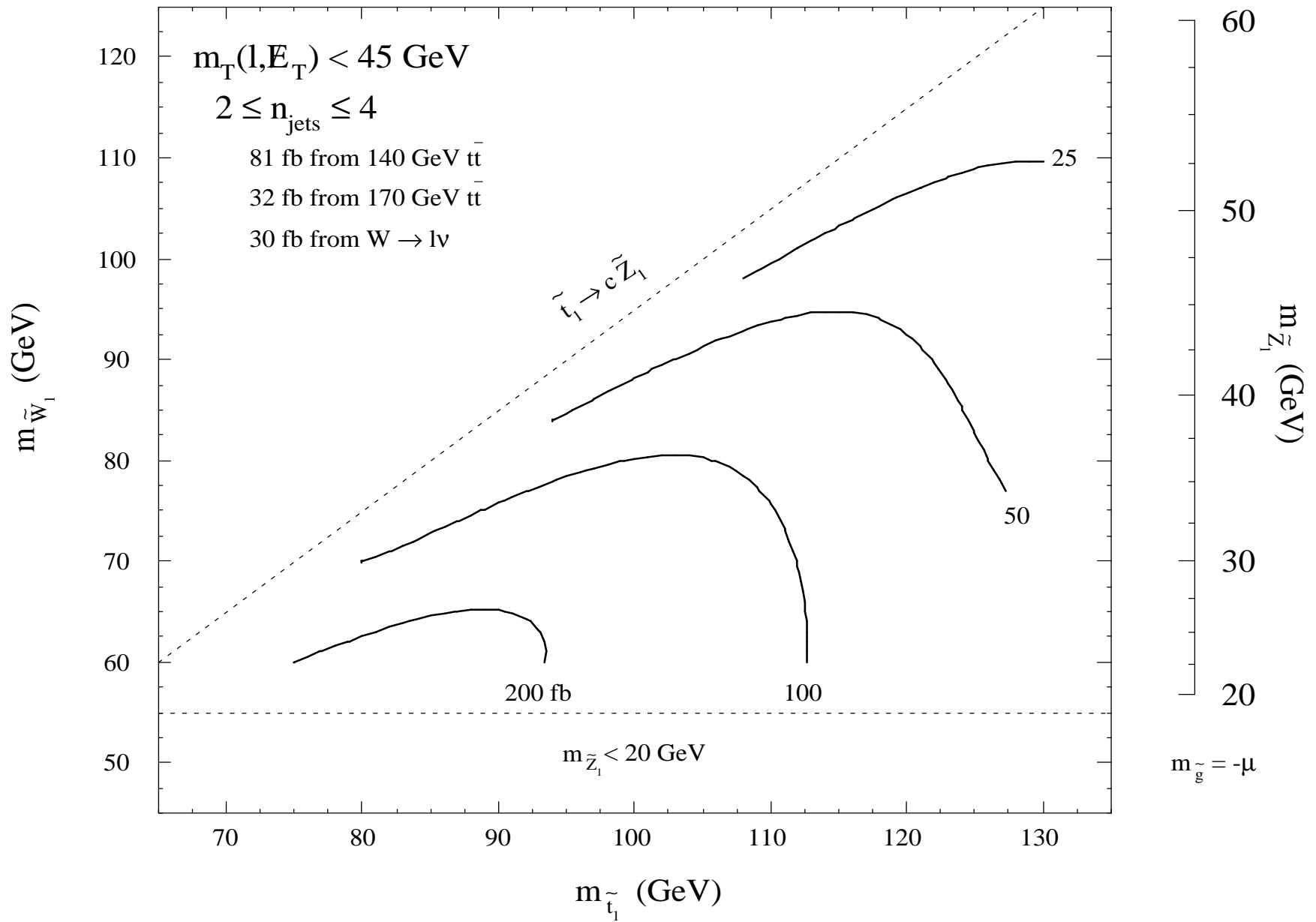


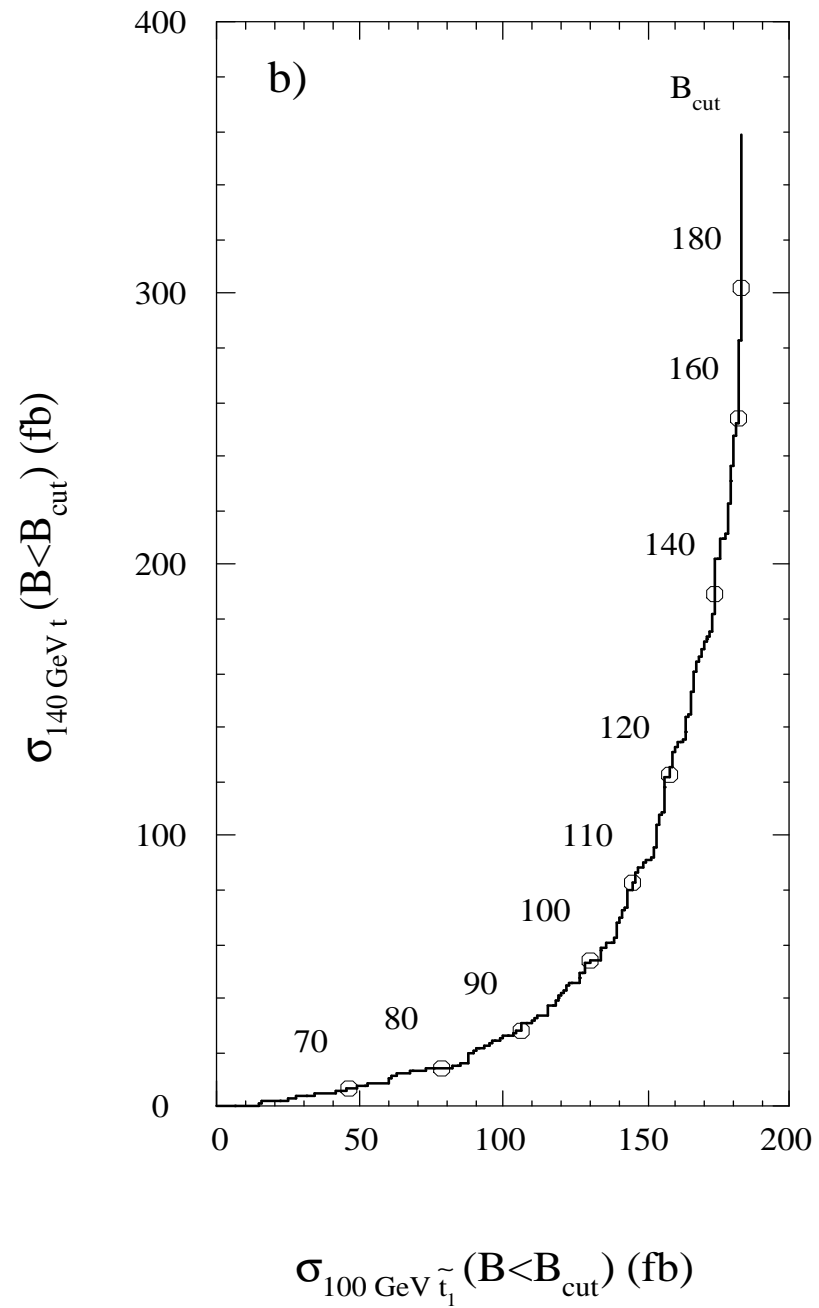
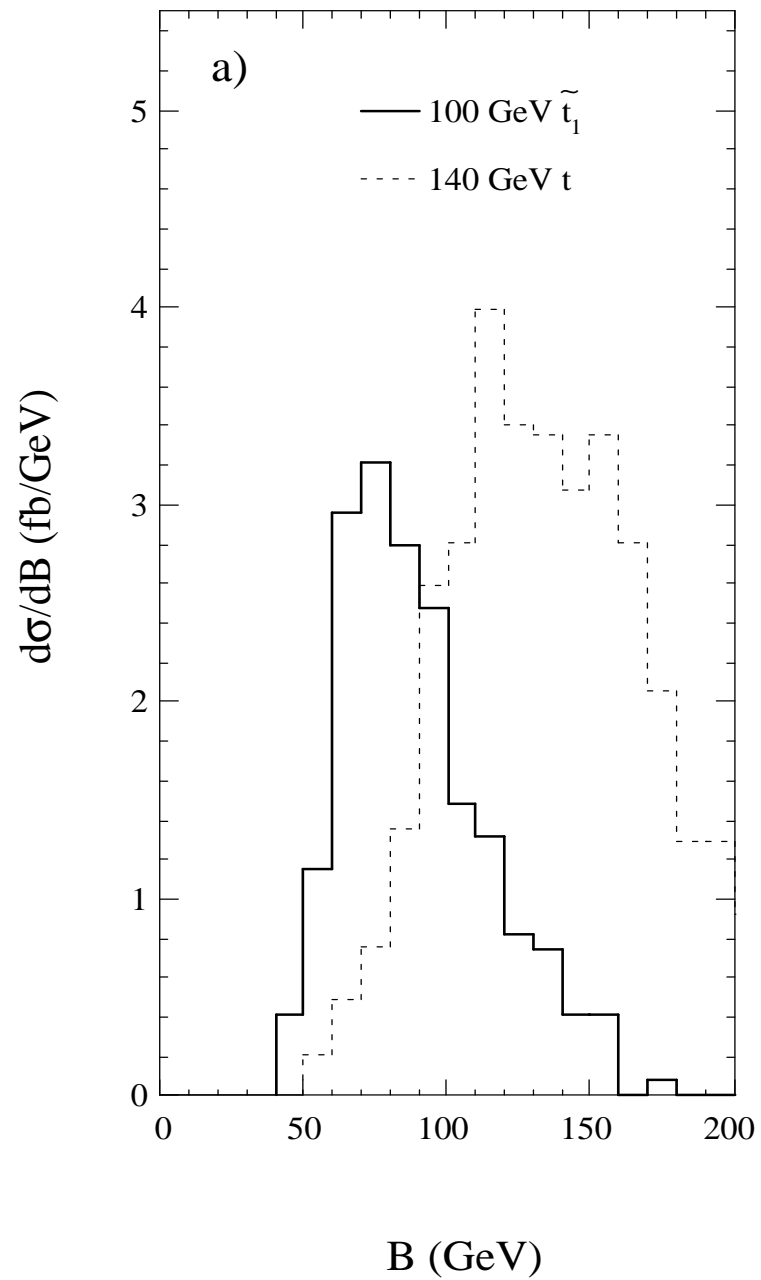
c-tag muon cross section for $\tilde{t}_1 \rightarrow c \tilde{Z}_1$ (fb)

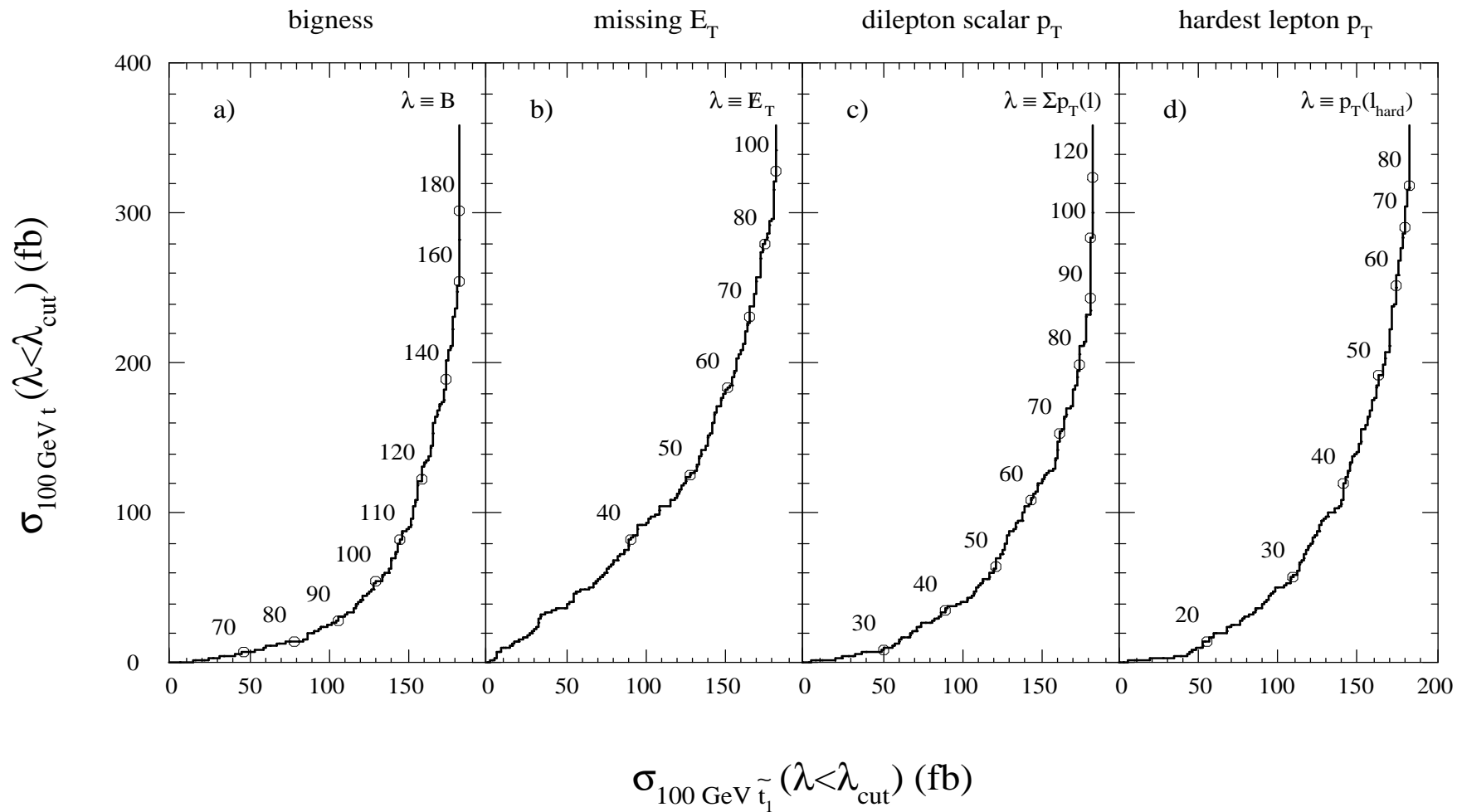


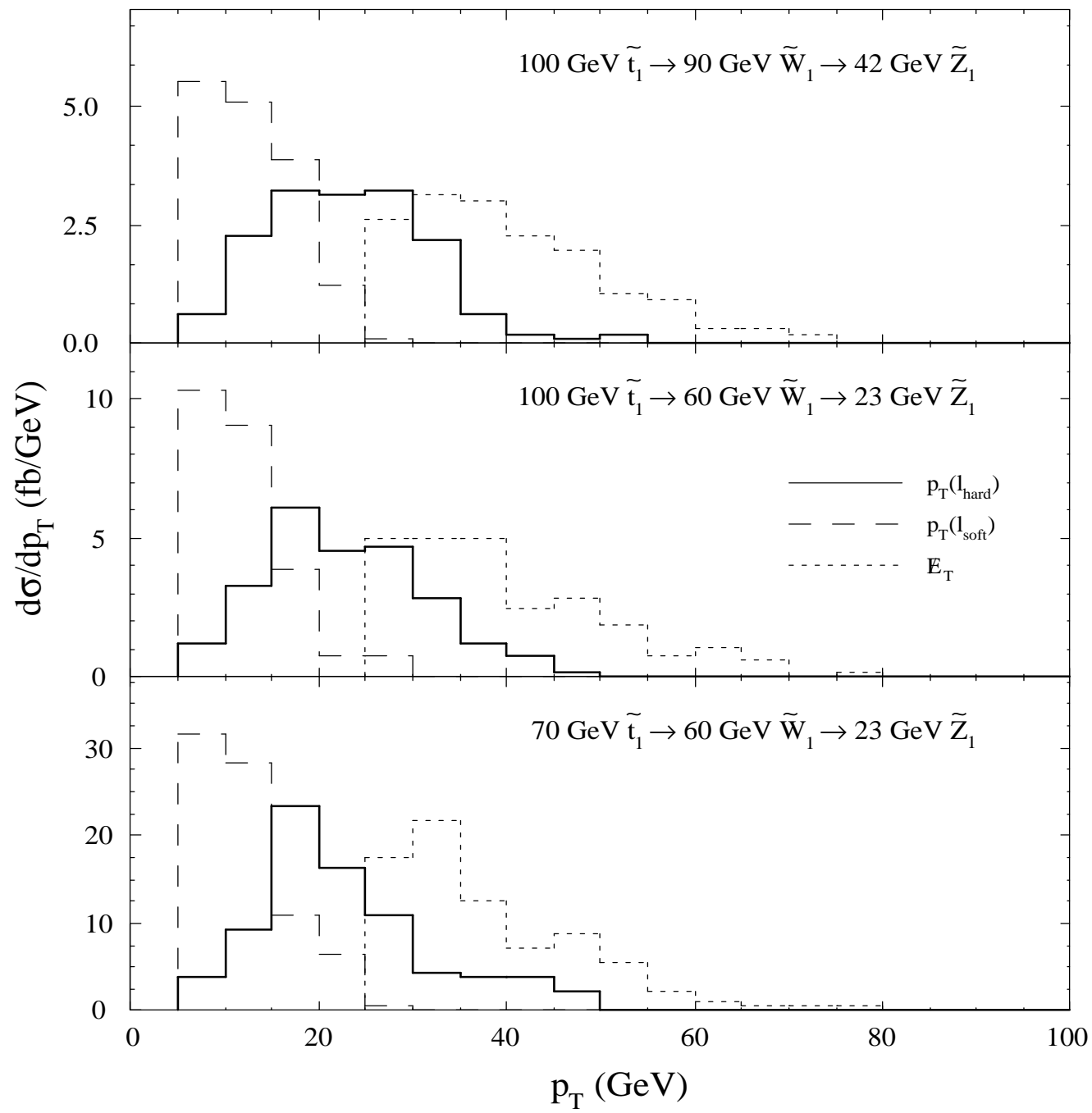


b-tagged single lepton cross section for $\tilde{t}_1 \rightarrow b \tilde{W}_1$ (fb)









dilepton cross section for $\tilde{t}_1 \rightarrow b \tilde{W}_1$ (fb)

